UNDERSÖKNINGSRAPPORT

1992:33

Free Convection along a Vertical Wall with Uniform Temperature

Yonghui Jin

Enheten för ventilation
Tf enhetschef: Anders Jansson

ARBETS
MILJÖ
INSTITUTET
NATIONAL INSTITUTE OF OCCUPATIONAL HEALTH

Preface

This study has been performed as a complement to the graduate studies of Yonghui Jin at the National Institute of Occupational Health and the Royal Institute of Technology. It was initiated by the need to analyze free convective flows along vertical walls within the test chamber employed for experimental work with particle transport in turbulent buoyant plumes. We are grateful to professor Tor-Göran Malmström at the Royal Institute of Technology for pointing out this need.

Free convective flows along vertical walls are, moreover, significant for indoor air movement and contaminant transport and therefore of general interests in occupational hygiene. We believe this to merit the publication of the study.

Solna, October 1992

Anders Jansson

Abstract

Reported results from measurements of free convection along vertical walls with uniform temperatures have been summarized. The results on the laminar boundary layers are consistent and show good agreement with theory. However, most of the reported measurements on the turbulent boundary layers show deficiencies and they are consistent only in certain normalized forms. These results were analyzed and formulas for predicting the maximum velocity and volume flow rate in the turbulent boundary layer are proposed. Expressions for predicting maximum velocity and volume flow rate in the transition region were obtained from interpolation of the equations for laminar and turbulent boundary layers.

The proposed expressions are well suited for predicting the maximum velocity and the volume flow rate in a free convection boundary layer for air at room temperature (important to indoor thermal comfort assessment and energy conservation in buildings). The proposed expressions will also give a better estimation of the maximum velocity and volume flow rate in the turbulent boundary layers than the previous ones being used for ventilation design purposes.

Key words: boundary layer, flow, free convection, laminar, transition, turbulent, vertical wall.

Sammanfattning

Kallras vid fönster och vägg kan orsaka drag inomhus. Det kan också påverka luftströmningen i lokalen och därmed transporten av föroreningar.

Mätresultat för fri konvektion vid en vertikal vägg med jämn temperatur har sammanfattas. För laminär strömning, stämmer mätresultat bra med teori. Å andra sidan stämmer mätresultat bra bara i viss normaliserade form för turbulent strömning. Analyser av tillgängliga mätresultat har gett enkla utryck för beräkning av maximal lufthastighet och luftflöde i det turbulenta gränsskiktet. I övergångsområdet, har interpolation mellan utryck för laminär och turbulent strömning gett empiriska ekvationer för beräkning av flöde och maximal hastighet.

Resultatet från den här studien leder till ett enkelt sätt att beräkna maximal hastighet och luftflöde som sträcker sig från det laminära till det turbulenta området. De nya utrycken för det turbulenta området stämmer också bättre med mätresultat än de tidigare utryck vilka används i ventilationstekniska sammanhang.

Nyckel ord: fri konvektion, gränsskikt, kallras, laminär, turbulent, vägg, övergång.

CONTENTS

1 Introduction

In industrial workplaces and offices, there always exist temperature differences between the inner surfaces of the enclosures and the indoor air. This is due to the heat exchange between the building and its environment through the enclosures. The temperature difference between the wall and the indoor air will cause free convective flow along the wall due to the density difference in the air. The stream of the free convection along a wall will go either upwards or downwards depending on whether the wall surface temperature is higher or lower than the indoor air temperature.

The free convection along the vertical walls may have a great influence on the room air flow pattern. The change of flow pattern will affect air contamination transport as well as thermal comfort in the occupied zones. It will also have an effect on the heat exchange between the indoor air and the environment. Thus, the characteristics of free convective flows are important to air contamination distribution, thermal comfort and energy conservation in buildings.

In this paper, only the velocity profiles and volume flow rates in the free convection boundary layers on vertical walls will be considered.

2 Free convection along a vertical wall

As practical situations are usually quite complicated and unpredictable, assumptions are made to simplify the problem of free convection along walls. We consider a vertical flat plate with a uniform surface temperature, T_w, immersed in a medium also with a uniform temperature, T_∞. The density variations are small in the whole flow region and the Boussinesq approximation can be applied, i.e. the density in the governing equations for the flow motion can be considered constant, except in buoyancy terms.

In forced convection, the Reynolds number is usually used to describe the flow situation. It is generally accepted that the Rayleigh number can be used to describe the flow situation in free convection boundary layers on vertical walls. The Rayleigh number is the product of the Grashof number, Gr, and the Prandtl number, Pr

$$Ra = Gr \cdot Pr \tag{1}$$

The definitions of Gr and Pr are

$$Gr = \frac{\beta g \Delta T x^3}{\nu^2} \tag{2}$$

$$Pr = \frac{\nu}{\alpha} \tag{3}$$

where
β = thermal expansion coefficient,
ΔT = temperature difference between the vertical plate and its surroundings,
x = plate height,
ν = kinematic viscosity,
α = thermal diffusivity, defined as $\kappa/\rho c_p$ (c_p = specific heat, κ = thermal conductivity, ρ = density).

From experiments, it has been shown that the convective flow will no more be laminar when Ra exceeds 10^9 [2]. For air at 20 °C (Pr = 0.71), the convective flow will thus no more be laminar when Gr is greater than 1.4×10^9. Redegren and Wiberg [10] observed laminar convection for air at a Rayleigh number of 2×10^9 (Gr = 2.8×10^9) in the boundary layer, at least from the wall surface out to the distance of the velocity maximum. Cheesewright's measurements with air [1] showed that the transition from laminar to turbulent begins at Gr = 2×10^9 and ends at Gr = 1×10^{10}. More accurate measurements were done by Cheesewright and Ierokiopitis [2] with LDA (Laser Doppler Anemometry) in air. In their measurements, an early onset of transition was observed at about Gr = 0.8×10^9. The fully developed turbulent region was found to begin at Gr = 1.6×10^{10}. The critical Rayleigh number at which the free convection turns into turbulent will depend on disturbances from the ambient air. Redegren et al [10] obtained laminar flow at a relatively higher Rayleigh number due to their careful elimination of the disturbances from the ambient room air (for instance, their measurements did not start until 4 minutes after the person left the test room). The development of the free convective flow along a vertical wall is shown in Figure 1.

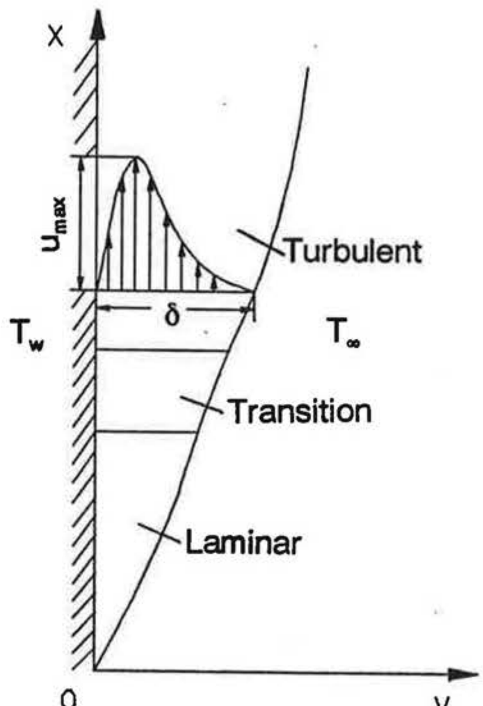

Figure 1. Development of free convective flow along a vertical wall

3 Laminar free convection boundary layer

A vertical wall immersed in a fluid of constant properties (except from density variations, which are important for buoyancy forces) will be taken into consideration. The flow is laminar and in steady state. The wall surface and the ambient fluid are at constant temperatures. The proper governing equations for describing the flow are shown in Appendix A. Early theoretical and experimental work was done by Schmidt and Beckman [12] on the laminar free convection boundary layer on a vertical wall with uniform temperature. Numerical solutions to the governing equations in similarity forms were developed by Ostrach with a refined method [9]. Nowadays the governing differential equations for laminar flow can be easily solved numerically on a personal computer. The governing equations in similarity forms and their solutions are listed in Appendix A. Measured values of the velocity profiles fit quite well with the numerical solutions, see Figure 2.

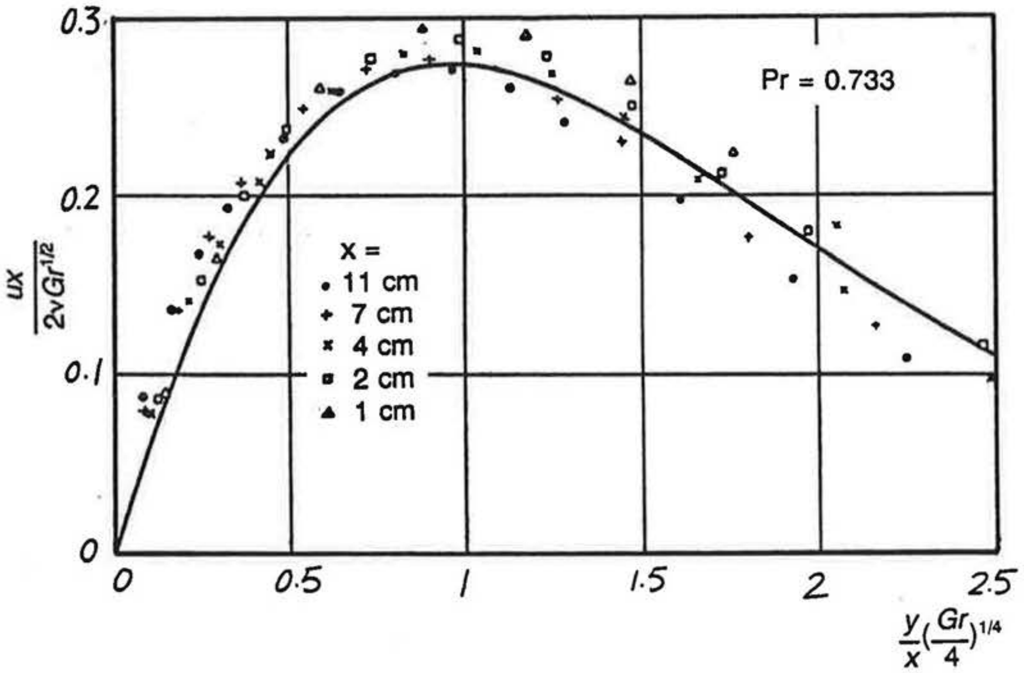

Figure 2. Measured velocity profile for the laminar boundary layer on a hot vertical flat wall in free convection, taken from [12].

The problem can also be approached by using the integral method (see Goldstein [5]), which gives approximate solutions to the problem. A certain velocity profile must be assumed in the boundary layer. Integration of the governing equations for the convective flow motion will then give a solution to the problem. This method makes it easier to study the influence of different parameters on the free convection. The method gives a solution within acceptable errors, if the velocity profile is properly chosen.

The velocity profile for the laminar boundary layer can be taken in the following form [5]

$$u = u_x \frac{y}{\delta}(1-\frac{y}{\delta})^2 \tag{4}$$

where u_x is a characteristic velocity which varies with wall height x.

Equation (4) and an additional equation for the assumed temperature profile can be put into the governing equations for the laminar free convection boundary layer to give an approximate solution to the problem [5]. The obtained characteristic velocity, u_x, and the boundary layer thickness, δ, are found to be

$$u_x = 5.17\nu(Pr+\frac{20}{21})^{-\frac{1}{2}}Gr^{\frac{1}{2}}x^{-1} \tag{5}$$

$$\delta = 3.93Pr^{-\frac{1}{2}}(Pr+\frac{20}{21})^{\frac{1}{4}}Gr^{-\frac{1}{4}}x \tag{6}$$

Combining equations (4), (5) and (6), we get the velocity profile in normalized form

$$\frac{u\,x}{2\nu Gr^{1/2}} = A(\frac{y}{x})(\frac{Gr}{4})^{\frac{1}{4}}[1-A(\frac{y}{x})(\frac{Gr}{4})^{\frac{1}{4}}]^2 \tag{7}$$

where

$$A = 0.36Pr^{\frac{1}{2}}(Pr+\frac{20}{21})^{\frac{1}{4}} \tag{8}$$

Comparison of the exact solution and the approximate solution to the velocity profile in a laminar free convection boundary layer at Pr = 0.71 is shown in Figure 3. The exact solution is taken from Appendix A. The figure illustrates the approximate nature of the integral method. However, the integral methods can provide algebraic solutions to the boundary layer equations, which facilitates analyses of the influence of different parameters when the exact solutions to the governing equations can only be obtained numerically.

Differentiating equation (4) gives the maximum velocity $u_{max} = 0.1481u_x$ at $y = \delta/3$ and u_{max} can be written as

$$u_{max} = 0.766\nu(Pr+\frac{20}{21})^{-\frac{1}{2}}Gr^{\frac{1}{2}}x^{-1} \tag{9}$$

For air at 20 °C (Pr = 0.71, $\nu = 15.1\times10^{-6}$ m^2/s), u_{max} becomes

$$u_{max} = 0.109\Delta T^{1/2}x^{1/2} \quad (m/s) \tag{10}$$

where
$\Delta T = |T_w - T_\infty|$, °C ($T_w$ = wall temperature, °C, and T_∞ = ambient air temperature, °C).
x = wall height, m.

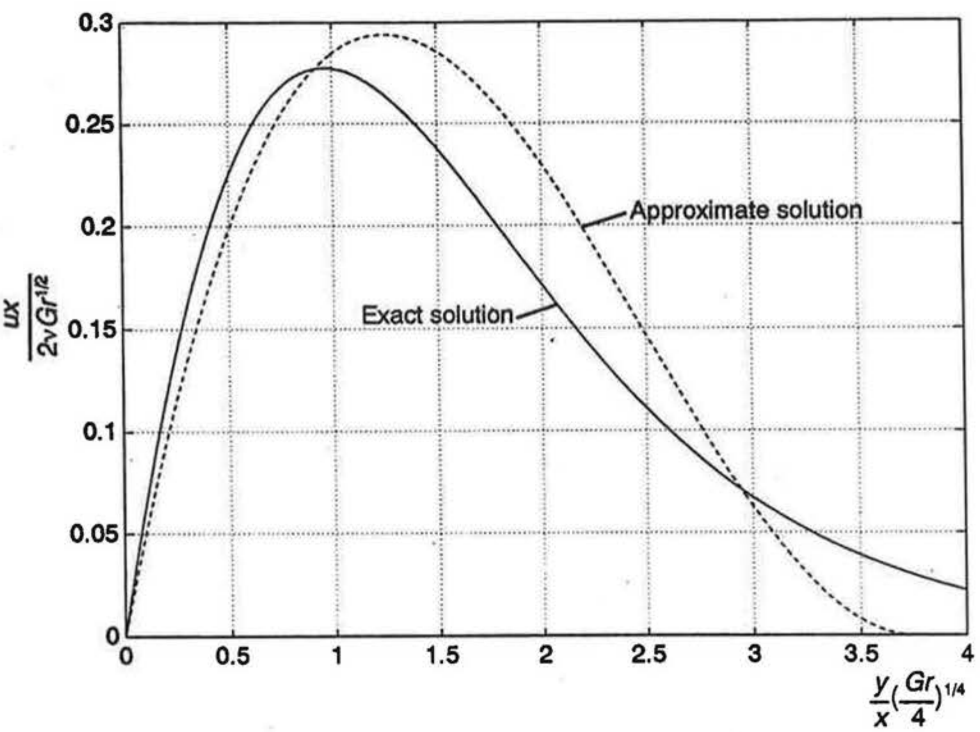

Figure 3. Velocity profile in a laminar free convection boundary layer at Pr = 0.71.

Integrating u in equation (7) from $y = 0$ to $y = \delta$, we get the volume flow rate per meter wall width, V, in the laminar boundary layer (for air at 20 °C)

$$V = 2.94\times10^{-3}\Delta T^{\frac{1}{4}}x^{\frac{3}{4}} \quad (m^3/s)/m \tag{11}$$

The numerical solution gives the maximum velocity, u_{max}, and the volume flow rate, V, at T_∞ = 20 °C as (see Appendix A)

$$u_{max} = 0.5546\nu Gr^{\frac{1}{2}}x^{-1} = 0.101\Delta T^{\frac{1}{2}}x^{\frac{1}{2}} \quad (m/s) \tag{12}$$

$$V = 1.702\nu Gr^{\frac{1}{4}} = 2.83\times10^{-3}\Delta T^{\frac{1}{4}}x^{\frac{3}{4}} \quad (m^3/s)/m \tag{13}$$

Redegren and Wiberg [10] carried out measurements of cold downward convection at windows. The flow was observed to be laminar at least out to the distance of the velocity maximum. Comparisons of the measured maximum velocities in the boundary layers and the calculated ones from equation (12) are shown in figure 4. It can be seen that the measured velocities fit quite well with the calculated values from equation (12).

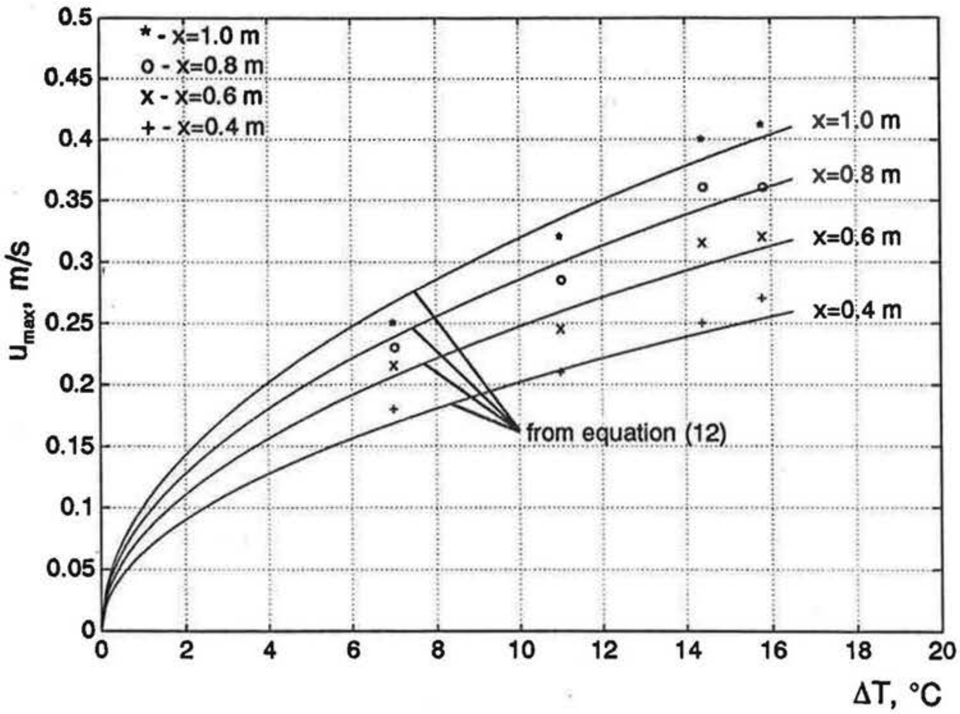

Figure 4. Measured maximum velocity in the boundary layer (from [10])

Comparisons of the measured volume flow rates in the boundary layer and the calculated ones from equation (13) are shown in Figure 5.

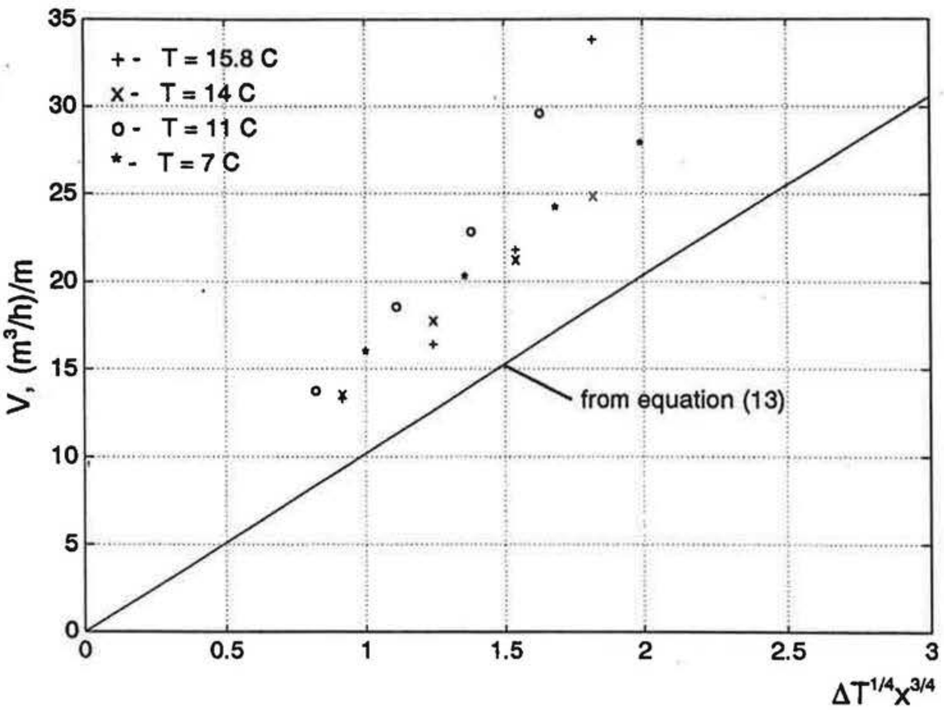

Figure 5. Measured volume flow rates in the laminar boundary layer (from [10])

The calculated values of the volume flow rates are considerably lower than the measured ones. This may be due to the inaccuracy in the velocity measurements, especially in the outer region of the boundary layer where the velocities were below 0.05 m/s. Notice also that the Rayleigh number reached up to 2×10^9 in their measurements. Thus the flow could have been in the transition region in the outer region of the boundary layer. In the transition region, more ambient air will be entrained into the boundary layer and thus the flow rate becomes larger.

4 Turbulent free convection boundary layer

The turbulent free convection boundary layer was first analyzed by Eckert and Jackson by using the integral method [3]. They used the 1/7th power-law velocity distribution in the forced boundary layer for the inner region and added an extra term to describe the outer region. Their assumed velocity profile is

$$u = u_x\left(\frac{y}{\delta}\right)^{\frac{1}{7}}\left(1-\frac{y}{\delta}\right)^4 \tag{14}$$

where u_x is a characteristic velocity in the boundary layer, varying with x.

The maximum velocity in the turbulent boundary layer, u_{max}, can be found by differentiating equation (14), which gives

$$u_{max} = 0.537u_x \quad (at\ y = \frac{\delta}{29}) \tag{15}$$

The volume flow rate per unit width in the turbulent boundary layer, V, can be obtained by integrating u from $y = 0$ to $y = \delta$

$$V = \int_0^\delta u\,dy = u_x\delta\int_0^1 \xi^{1/7}(1-\xi)^4 d\xi = 0.146u_x\delta \tag{16}$$

where $\xi = y/\delta$.

The boundary layer thickness, δ, and the characteristic velocity, u_x, were derived by Eckert and Jackson by introducing the shearing stress relation for forced convection on the wall and their results are [3]

$$\delta = 0.565xGr^{-\frac{1}{10}}Pr^{-\frac{8}{15}}[1+0.494Pr^{\frac{2}{3}}]^{\frac{1}{10}} \tag{17}$$

$$u_x = 1.185\frac{\nu}{x}Gr^{\frac{1}{2}}[1+0.494Pr^{\frac{2}{3}}]^{-\frac{1}{2}} \tag{18}$$

From equations (16), (17) and (18), we get the volume flow rate per unit width in the turbulent boundary layer

$$V = 0.098\nu(Pr)^{-\frac{8}{15}}[1+0.494(Pr)^{\frac{2}{3}}]^{-\frac{4}{10}}Gr^{\frac{4}{10}} \tag{19}$$

For air at 20 °C (Pr = 0.71 and $\nu = 15.1\times10^{-6}$ m^2/s), equations (15) and (19) become

$$u_{max} = 0.099\Delta T^{\frac{1}{2}}x^{\frac{1}{2}} \quad (m/s) \tag{20}$$

$$V = 2.88\times10^{-3}\Delta T^{0.4}x^{1.2} \quad (m^3/s)/m \tag{21}$$

where
x = wall height, m,
ΔT = temperature difference between the wall and the room air, °C.

Notice that equation (20) gives almost the same value for the maximum velocity as equation (12) for the laminar boundary layer. However, the errors caused by using the integral method can only be determined from comparison with experimental results, since there is no exact solution for the turbulent free convective flow.

As the boundary layer thickness is rather difficult to determine, a displacement thickness, δ^*, is often used for characterizing the boundary layer thickness. This thickness is defined as

$$\delta^* = \int_0^\infty \frac{u}{u_{max}}dy \tag{22}$$

The velocity profile in normalized form can be obtained by combining equations (14), (15) and (22)

$$\frac{u}{u_{max}} = 1.862\left(\frac{y}{3.67\delta^*}\right)^{\frac{1}{7}}\left(1-\frac{y}{3.67\delta^*}\right)^4 \tag{23}$$

A number of measurements of the turbulent free convection boundary layer were done by several authors in the late 60's, see e.g. Cheesewright [1], Lock and Trotter [7], Vliet and Liu [13]. The velocity profiles normalized in u/u_{max} are consistent with each other and Eckert and Jackson's profile showed rather good agreement with the measured results (see [13]). However, there are large discrepancies between Eckert and Jackson's velocity profile and the experimentally obtained velocity profile normalized as $u/(g\Delta Tx/T_\infty)^{1/2}$, see Figure 6.

More work should be done to determine the actual velocity profile. Mason and Seban [8] employed a simple turbulence model to solve the governing equations for the turbulent free convection boundary layer. The calculated velocity profile was in general accordance

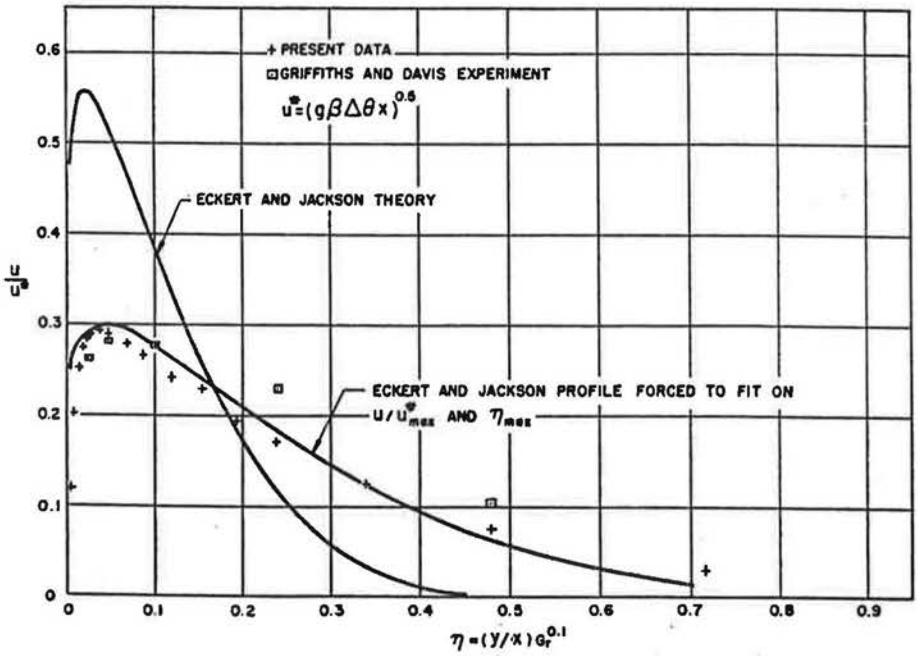

Figure 6. Velocity profile in the turbulent boundary layer (from Cheesewright [1]).

with the forms of data obtained by Cheesewright and the maximum velocity is about 25% higher than that in Cheesewright's data. Hoogendoorn and Euser [6] showed that although the data from different experiments seemed to be consistent, they did not satisfy an integral energy balance, i.e. the heat transferred to the boundary layer calculated from the velocity and temperature profiles at some height did not agree with the heat transfer from the wall. They suggested the source of errors lay in the mean velocity data. This was confirmed when Cheesewright and Ierokiopitis [2] carried out more accurate measurement on the velocity profile in the turbulent boundary layer with LDA (Laser Doppler Anemometry). The obtained velocity profiles by these authors are shown in Figure 7.

The figure shows a relatively good agreement between the results from different authors. Mason and Seban's data shows higher maximum velocity than the others and the velocity data from Hoogendoorn and Euser shows some deviation in the low velocity region. This may be due to the disturbances from the ambient and different methods of the velocity measurement.

The maximum velocity in Cheesewright and Ierokiopitis's data is at $(y/x)\mathrm{Gr}^{0.1} = 0.053$

$$u_{max} = 0.349\nu Gr^{1/2}x^{-1} \tag{24}$$

Eckert and Jackson's profile can be forced to fit the maximum velocity in Cheesewright and Ierokiopitis's data and the forced profile fits very well the measured data (see Fig. 7). The velocity profile obtained by forcing u_{max} to fit the measured data is

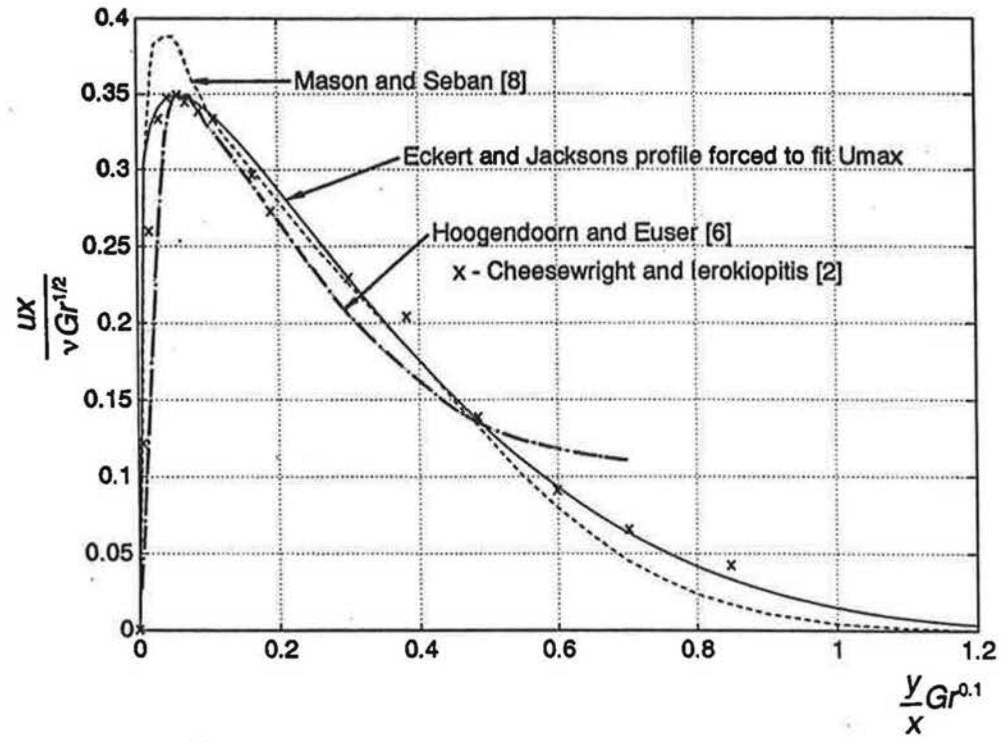

Figure 7. Velocity profile in the turbulent boundary layer (data from [2], [6] and [8])

$$\frac{u\,x}{\nu Gr^{1/2}} = 0.650\left(\frac{y}{1.656xGr^{-0.1}}\right)^{\frac{1}{7}}\left(1-\frac{y}{1.656xGr^{-0.1}}\right)^{4} \tag{25}$$

The volume flow rate per unit wall width in the boundary layer, V, can be obtained by integrating u from $y = 0$ to $y = \delta$,

$$V = 0.157\nu Gr^{0.4} \tag{26}$$

For air at 20 °C, equations (24) and (26) can be further simplified to

$$u_{max} = 0.064\Delta T^{\frac{1}{2}}x^{\frac{1}{2}} \quad (m/s) \tag{27}$$

$$V = 4.38\times10^{-3}\Delta T^{0.4}x^{1.2} \quad (m^3/s)/m \tag{28}$$

Notice that the application of equations (24)-(28) should be restricted to turbulent free convection in air at reasonably large Grashof numbers, since measured results were not carried out for a wide range of Grashof numbers.

5 The transition region

As the convective flow rises along an isothermal vertical wall, the Gr number is increasing with the wall height x. The laminar flow will eventually become turbulent at some height. The turbulence begins gradually over a transition region. So far, very few measurements concerning the velocity profile in the boundary layer during transition have been done. The onset of the transition is also strongly influenced by the external disturbances. However, an approximation for engineering use in the transition region may be obtained by interpolating between the laminar and turbulent regions. For convenience, we assume that the transition starts at Gr = 1×10^9 and ends at Gr = 1×10^{10} for air. The maximum velocity and volume flow rate in the transitional boundary layer may be obtained by interpolating between these two starting and ending Gr numbers from equations (12), (13), (24) and (26), see Figures 7 and 8.

The obtained maximum velocity and volume flow rate per unit wall width in the boundary layer during transition from interpolation are

$$u_{max} = 35.7 \nu Gr^{0.299} x^{-1} \tag{29}$$

$$V = 1.11 \times 10^{-4} \nu Gr^{0.715} \tag{30}$$

For air at 20 °C, equations (29) and (30) can be further simplified to

$$u_{max} = 0.149 \Delta T^{0.299} x^{-0.103} \quad (m/s) \tag{31}$$

$$V = 1.16 \times 10^{-3} \Delta T^{0.715} x^{2.14} \quad (m^3/s)/m \tag{32}$$

The obtained constants in equations (29) - (32) are dependant on the choice of the starting and ending Gr numbers of the transition region. What the equations (29) - (32) give are just an approximation of the maximum velocity and volume flow rate in our defined "transition region". They may have lost their physical meaning.

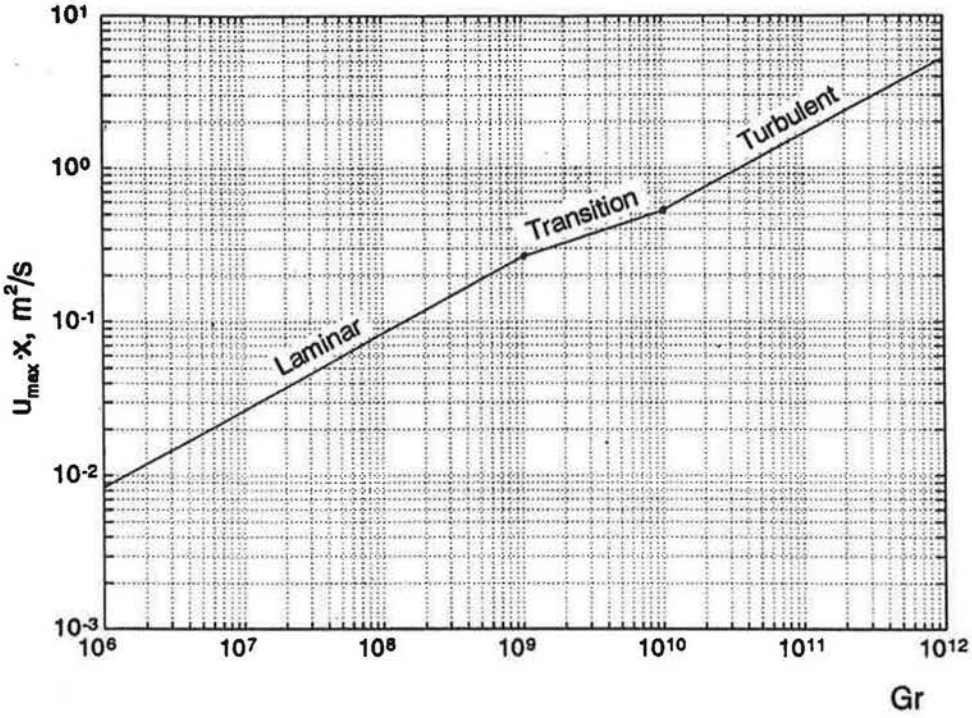

Figure 8. Variations of maximum velocity in the free convection boundary layer with Grashof number

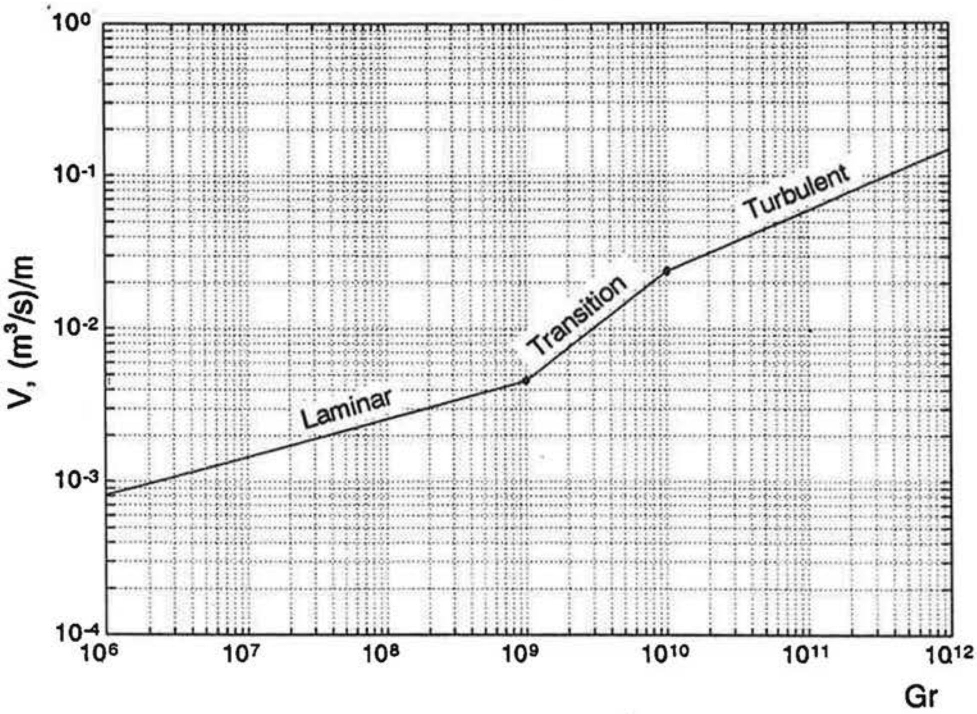

Figure 9. Variation of flow rate in the free convection boundary layer with increasing Grashof number.

6 Free convection along vertical walls in buildings

In winter time, there is cold downward convection along inner surfaces of the windows and the outer walls and in summer time the convective flow will go upwards. The intensity of the free convection will depend on the temperature difference between the wall surface and indoor air, and the height of the wall. When the outdoor temperature is -20°C and the indoor air temperature is 20°C, the temperature differences are the following according to Rydberg [11].

Table 1. The temperature differences between the enclosure surface and the room air and the corresponding Grashof number at different heights.

Enclosure type	T_∞-T_w, °C	Gr (x=1m)	Gr (x=2m)	Gr (x=3m)
2-glass window (k=2.5)	13.0	1.9×10^{9}	1.5×10^{10}	5.1×10^{10}
3-glass window (k=1.7)	8.7	1.2×10^{9}	1.0×10^{10}	3.4×10^{10}
wall (k=1.0)	5.2	7.6×10^{8}	6.1×10^{9}	2.0×10^{10}
wall (k=0.3)	1.6	2.3×10^{8}	1.8×10^{9}	2.3×10^{9}

Note: k is the coefficient of heat exchange, W/m²·°C.

From the table, we can see that the free convection will no more be laminar when the window height is greater than 1 m and when the wall height is greater than 2 m. However, as the values given in Table 1 is for extreme cold winter days, most free convection will be in the transition region.

A summary of the equations for predicting the maximum velocity and volume flow rates in the free convection boundary layer at T_∞ = 20 °C is listed in table 2.

Table 2. Summary of equations for predicting u_{max} and V (per meter wall width) at T_∞ = 20°C.

Flow situation	u_{max}, m/s	V, (m³/s)/m
Gr < 10^9	$0.101\ \Delta T^{0.5}x^{0.5}$	$2.83\times10^{-3}\ \Delta T^{0.25}x^{0.75}$
10^9< Gr <10^{10}	$0.149\ \Delta T^{0.299}x^{-0.103}$	$1.16\times10^{-3}\ \Delta T^{0.715}x^{2.14}$
Gr > 10^{10}	$0.064\ \Delta T^{0.5}x^{0.5}$	$4.38\times10^{-3}\ \Delta T^{0.4}x^{1.2}$

Calculated maximum velocities and volume flow rates for different heights and temperature differences are shown in Figures 10 and 11.

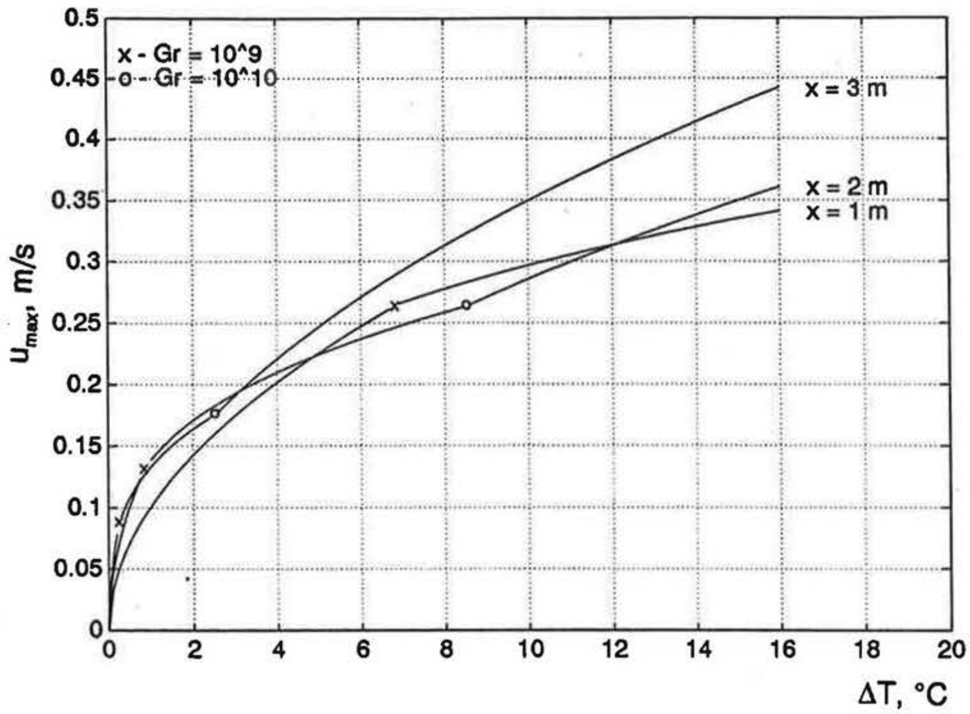

Figure 10. Maximum velocities in the free convection boundary layers

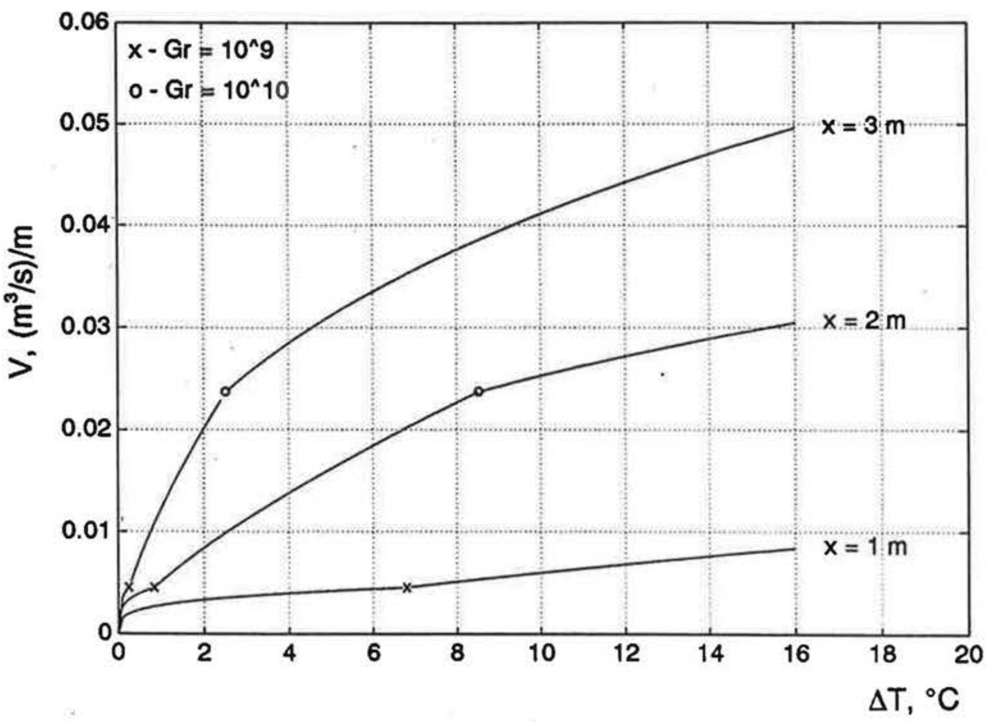

Figure 11. Volume flow rates in the free convection boundary layers

7. Conclusions

There are proper solutions to the governing equations for laminar free convection boundary layers on an isothermal vertical wall. The solutions are in good agreement with reported results from measurements.

For the turbulent free convection boundary layer, a typical approximate solution based on the integral method was given by Eckert and Jackson. However, their solution showed large discrepancies compared with measured results. Recent more accurate measurements on the turbulent boundary layer have been used for obtaining better formulas for predicting maximum velocity and volume flow rate. Further measurements are still needed for the turbulent free convection boundary layer.

Due to the instabilities in the boundary layer during transition, no deterministic solutions exist or may be expected. However, approximate expressions for engineering purposes may be found by interpolating between the laminar and turbulent boundary layers. The obtained expressions can be used for estimating the air flow in the transition boundary layer.

The free convection along a window or wall in a room is often in the transition region or the turbulent region. The maximum velocity and volume flow rate in the free convection boundary layer can be predicted once the wall height and the temperature difference are known.

References

[1] Cheesewright R. Turbulent free convection from a vertical plane surface. Journal of Heat Transfer 90:2 (1968). pp. 1-8.

[2] Cheesewright R, Ierokiopitis E. Velocity measurement in a turbulent convection boundary layer. International heat transfer conference, Munich (1982). Paper NC31.

[3] Eckert ERG, and Jackson T. Analysis of turbulent free-convection boundary layer on a flat plate. NACA Report 1015 (1951).

[4] Ede AJ. Advances in free convection. Advanced Heat Transfer 4 (1967). pp. 1-64.

[5] Goldstein S. Modern Developments in Fluid Dynamics 2 (1938). pp. 638-643.

[6] Hoogendoorn CJ. Velocity profiles in the turbulent free convection boundary layer. International Heat Transfer Conference, Toronto (1978). Paper NC-2.

[7] Lock GSH, Trotter FJ. Observation on the structure of a turbulent free convection boundary layer. International Journal of Heat and Mass Transfer 11 (1968). pp. 1225-1232.

[8] Mason HB, Seban RA. Numerical prediction for turbulent free convection from vertical surfaces. International Journal of Heat and Mass transfer 17 (1974). pp. 1329-1336.

[9] Ostrach S. An analysis of laminar free-convection flow and heat transfer about a plate parallel to the direction of the generating body force. NACA Report 1111 (1953).

[10] Redegren N, Wiberg T. Kallras - en experimentell undersökning, Tekniska Meddelande 20 (1972), Department of Heating and Ventilation, Royal Institute of Technology, Stockholm.

[11] Rydberg J. Kallras vid fönster. VVS 34 (11) (1963). pp. 411-413.

[12] Schmidt E, Beckman W. Das Temperatur- und Geschwindigkeitsfeld von einer Wärme abgebenden senkrechten Platte bei natürlicher Konvektion, Forsch-Ing.-Wes. 1 (1930). pp. 391-406.

[13] Vliet GC, Liu CK. An experimental study of turbulent natural convection boundary layers. Journal of Heat Transfer 91 (1969). pp. 517-531.

Appendix A.

The governing equations for the free convection boundary layer on a vertical plate are [5]

$$\frac{\partial u}{\partial x}+\frac{\partial v}{\partial y} = 0 \qquad \text{(A-1a)}$$

$$u\frac{\partial u}{\partial x}+v\frac{\partial u}{\partial y} = \nu_{\infty}\frac{\partial^2 u}{\partial y^2}+g\frac{\rho_{\infty}-\rho}{\rho_{\infty}} \qquad \text{(A-1b)}$$

$$u\frac{\partial T}{\partial x}+v\frac{\partial T}{\partial y} = \frac{\nu_{\infty}}{Pr}\frac{\partial^2 T}{\partial y^2} \qquad \text{(A-1c)}$$

and the boundary conditions are

$$u_{y=0} = v_{y=0} = 0,\ u_{y=\infty} = 0,\ T_{y=\infty} = T_{\infty},\ T_{y=0} = T_w \qquad \text{(A-1d)}$$

The governing equations of the boundary layer conditions can be transformed into similarity forms by setting

$$\eta = \frac{y}{x}\left(\frac{Gr}{4}\right)^{\frac{1}{4}} \qquad \text{(A-2a)}$$

$$\psi(x,y) = 4\nu\left(\frac{Gr}{4}\right)^{\frac{1}{4}}f(\eta) \qquad \text{(A-2b)}$$

$$\frac{T-T_{\infty}}{T_w-T_{\infty}} = \theta(\eta) \qquad \text{(A-2c)}$$

where ψ is the stream function and u can written as a function of ψ as

$$u = \frac{\partial\psi}{\partial y} = 2\nu Gr^{\frac{1}{2}}x^{-1}f'(\eta) \qquad \text{(A-3)}$$

Equations (A-1a,b,c) can then be reduced to

$$f'''+3ff''-2(f')^2+\theta = 0 \qquad \text{(A-4a)}$$

$$\theta''+3Prf\theta' = 0 \qquad \text{(A-4b)}$$

The boundary conditions become

$$f_{\eta=0} = 0,\ f'_{\eta=0} = 0,\ \theta_{\eta=0} = 1,\ f'_{\eta=\infty} = 0,\ \theta_{\eta=\infty} = 0 \qquad \text{(A-4c)}$$

The velocity and temperature profiles can thus be obtained if f' and θ can be solved from equations (A-4a), (A-4b) and (A-4c).

An ODE (ordinary differential equation) solver (PC-Matlab from the MathWorks, Inc.) on a personal computer was used to solve the ordinary differential equations numerically. The boundary conditions $f'_{\eta=\infty} = 0$ and $\theta_{\eta=\infty} = 0$ can not be used directly in solving the equations. Values must be found both for $f''_{\eta=0}$ and $\theta'_{\eta=0}$ so that the solution satisfies $f'_{\eta=\infty} = 0$ and $\theta_{\eta=\infty} = 0$. Solutions to the different equations satisfying these boundary conditions are shown in Figure A-1.

The initial values for f'' and θ' were found $f''_{\eta=0} = 0.67745$ and $\theta'_{\eta=0} = -0.50208$. The maximum value for f' is 0.2773 at $\eta = 0.9705$. The maximum velocity, u_{max}, is

$$u_{max} = 0.5546 \nu Gr^{\frac{1}{2}} x^{-1} \quad \text{(A-5)}$$

Integrating f' from $\eta = 0$ to $\eta = \infty$ gives a value of 0.6018, thus we have the volume flow rate per unit boundary layer width, V

$$V = \int_0^\infty u dy = 2\sqrt{2}\nu Gr^{\frac{1}{4}} \int_0^\infty f'(\eta) d\eta = 1.7021 \nu Gr^{\frac{1}{4}} \quad \text{(A-6)}$$

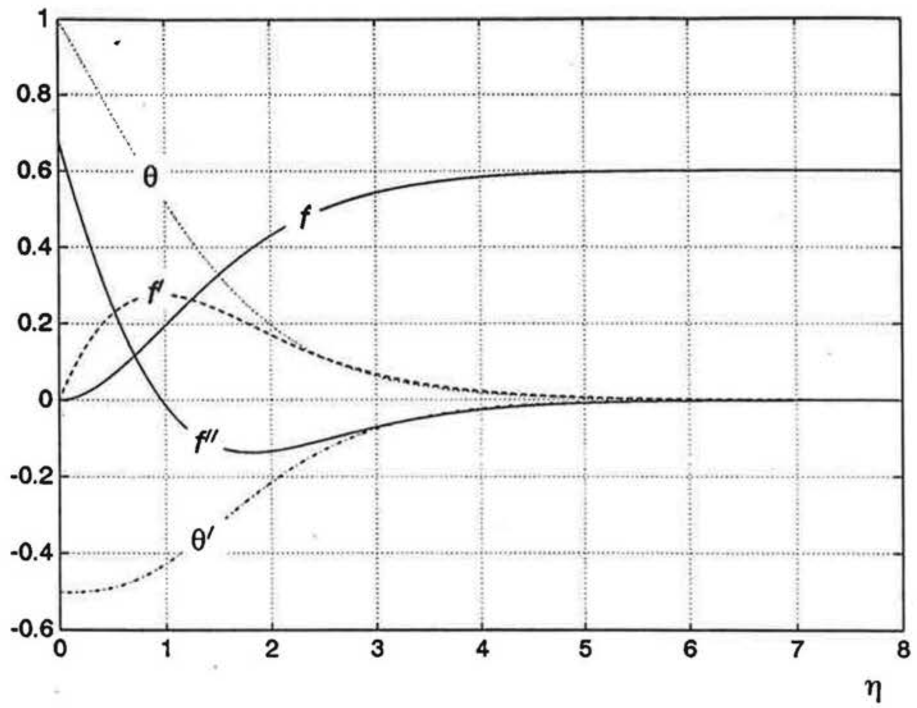

Figure A-1. Solutions to equations (A-4a), (A-4b) and (A-4c) for Pr = 0.71.

UNDERSÖKNINGSRAPPORTER

1992:8 **Kemisk karaktärisering av rök från termiskt sönderdelade plaster.** J Scullman, B-O Lundmark och C Östman.

1992:9 **Rehabiliteringsresultat för patienter med nack- och/eller skulderbesvär ett respektive två år efter påbörjad rehabilitering.** M Marklund och K Nilsson samt Y Bragner, A Hedström, I Jensen, B Jonsson, Å Nygren, B Salén, E Sprangfort och P Westerholm.

1992:10 **Yrkeshygieniska risker vid ytbehandling i träindustrin. Delrapport 1: Appliceringsmetoder och ytbehandlingsmaterial.** M Hultengren, G Rosén och B von Tell.

1992:11 **Akademiker under 90-talet. En studie av SACO-medlemmarnas arbetsvillkor.** G Aronsson, A Lantz och G Westlander.

1992:12 **Personburna och bärbara direktvisande instrument för mätning av gasformiga föroreningar i arbetsmiljön – en marknadsöversikt.** L Hansén och I Skare.

1992:13 **Arbetsmiljöaspekter i statliga myndigheters datoriseringsprojekt. En studie om användningen av policyskriften "Bildskärmsarbete och arbetsmiljö".** W Astvik.

1992:14 **Bestämning av diffusionskonstanter i gasfas.** A Bemgård och A Colmsjö.

1992:15 **Ett psykosocialt utvecklingsprogram och dess genomförande. En delstudie inom forskningsprojektet.** O Frieberg och B-I Andersson.

1992:16 **Accidents Encountered in High Risk Occupational Groups of a Swedish Automobile and Truck Factory: Their Most Common Circumstances and Consequences.** L Laflamme.

1992:17 **Inomhusmiljö och hälsa bland kontorsarbetare i Västerbotten. Studiens bakgrund, syfte och uppläggning.** B Stenberg, K Hansson Mild, G Lönnberg, M Sandström, J Sundell och S Wall.

1992:18 **Inomhusmiljö och hälsa bland kontorsarbetare i Västerbotten. Inomhusklimat, byggnader och rum. Del 1: Bakgrund och tekniska data.** J Sundell.

1992:19 **Inomhusmiljö och hälsa bland kontorsarbetare i Västerbotten. Inomhusklimat, byggnader och rum: Del 2: Fall- referentstudier av sjukahus-syndromet (SBS) och hudbesvär bland bildskärmsarbetare.** J Sundell, T Lindvall och B Stenberg.

1992:20 **Biologisk kontroll vid yrkesmässig exponering för stenkolstjära.** J-O Levin, E Sikström och M Rhén.

1992:21 **Partikulära luftföroreningar i ett allergianpassat och två konventionella daghem.** B Christensson och S Krantz.

1992:22 **Hälsorisker i arbete vid elproduktion och eldistribution. Delrapport 11: Hälsotillståndet vid treårsuppföljningen.** S Törnqvist, R-M Högström, F Gamberale och B Knave.

1992:23 **Ergonomic parameters for the driver's workplace. A. Maximum ability to twist the body. B. Maximum force exerted on hand controls and pedals. C. Working range in operation of hand controls.** J-E Hansson, S Kihlberg, L Andersson, M Aoki, S Carlsöö, M Friberg, A Isaksson och T Wilhelmi.

1992:24 **Kvalifikationskrav av relationskaraktär. En metodstudie grundad på situationskritiska händelser i två yrken: barnskötare och förskollärare.** I Paulsson.

1992:25 **Lungröntgenstudie avseende lungfunktion och lungröntgen på Rönnskärsarbetare med lång tids exponering för lungtoxiska ämnen.** N Stjernberg, M-C Ledin, G Lindén, V Englyst och B Kolmodin-Hedman.

1992:26 **Exponering för ammoniak som injicerats i halm.** L Juringe.

1992:27 **Basenhetsorganisation. En studie av ett förändringsarbete inom sjukvården.** B Pingel och H Robertsson.

1992:28 **Om context-orienterad ansats. En metoddiskussion med anknytning till organisationspsykologisk forskning.** G Westlander.

1992:29 **NOSA Aerosolsymposium Solna 27-28 oktober 1992.** G Lidén och A Jansson (red).

1992:30 **Störningsupplevelse och obehag vid exponering för buller från ultraljudskälla.** K Holmberg, U Landström och B Nordström.

1992:31 **Akademikers arbetsvillkor. Jämförelser mellan SACO-förbunden.** B Cocke-Spalloni och A Strömberg.

1992:32 **I väntan på åtgärder. En interventionsorienterad studie av bildskärmsoperatörer i arbete av rutinkaraktär.** G Westlander, E Viitasara, H Shahnavaz och A Johansson.

1992:33 **Free Convection along a Vertical Wall with Uniform Temperature.** Y Jin.